Electronic Supplementary Material (ESI) for Journal of Materials Chemistry A. This journal is © The Royal Society of Chemistry 20XX

Optimized electron/ion transport by constructing radially oriented channels in MXene hybrid fiber electrodes for high-performance supercapacitors at low temperatures

Tianyu Zhao,[a,b] Dongzhi Yang,[a,*] Shu-Meng Hao,[a] Ting Xu,[b] Ming Zhang,[b] Weidong Zhou[a] and Zhong-Zhen Yu[a,b*]

[a] State Key Laboratory of Organic-Inorganic Composites, College of Materials Science and Engineering, Beijing University of Chemical Technology, Beijing 100029, China.

E-mail: yangdz@mail.buct.edu.cn

[b] Beijing Key Laboratory of Advanced Functional Polymer Composites, Beijing University of Chemical Technology, Beijing, 100029, China.

E-mail: yuzz@mail.buct.edu.cn

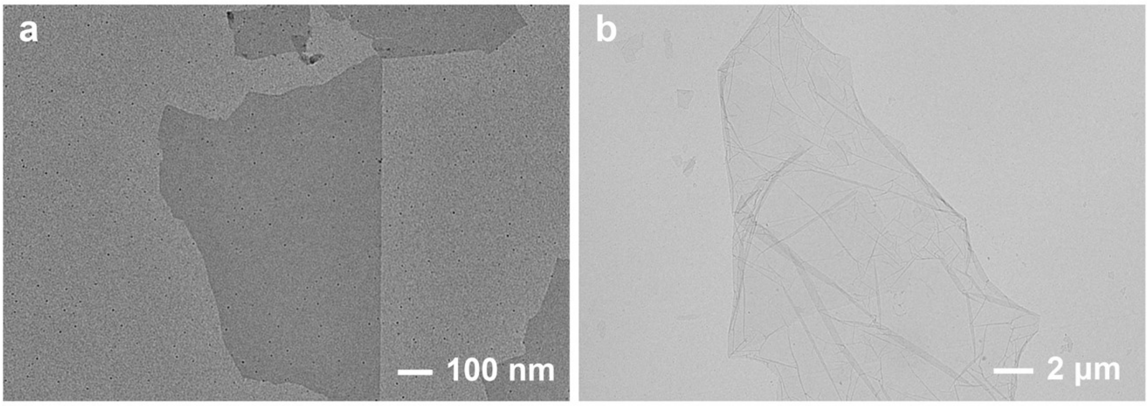

Fig. S1. TEM images of (a) $Ti_3C_2T_x$ nanosheets and (b) GO nanosheets.

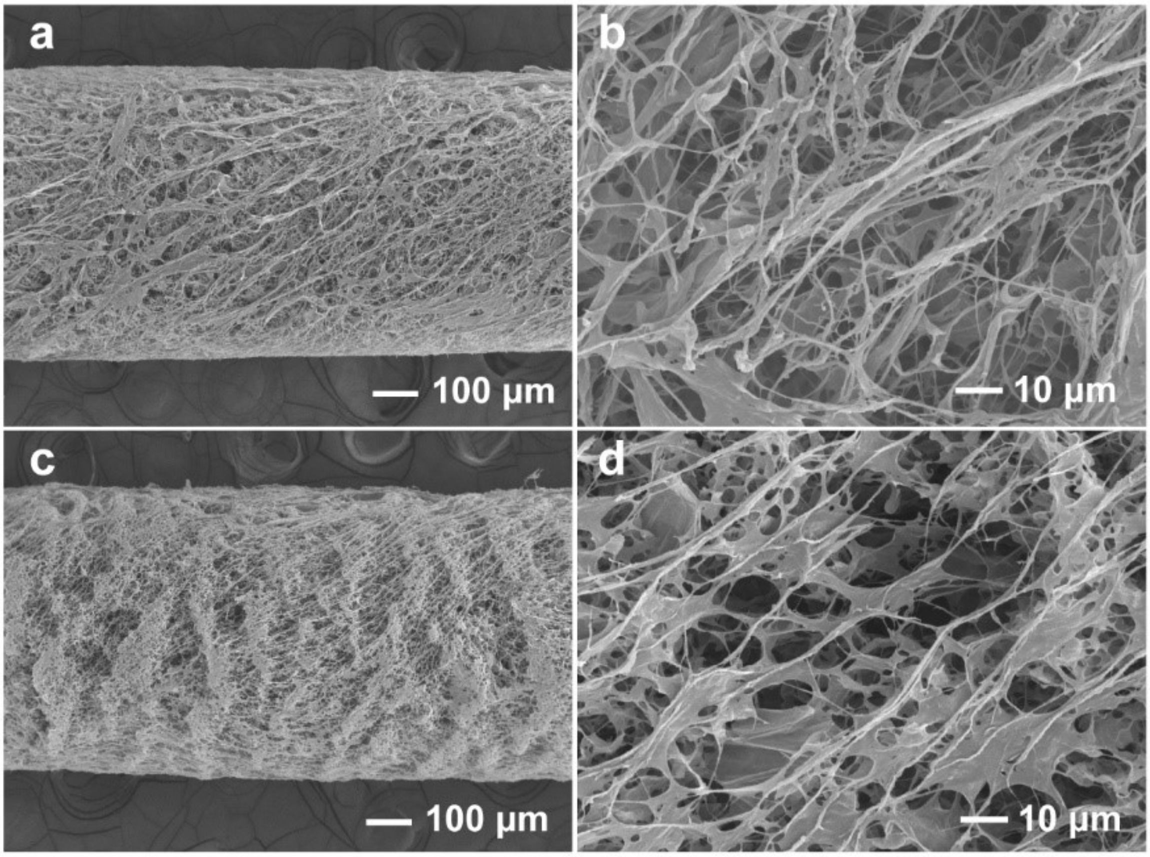

Fig. S2. SEM images of the surface structures of (a, b) U-MGP_3 and (c, d) D-MGP_3 fibers.

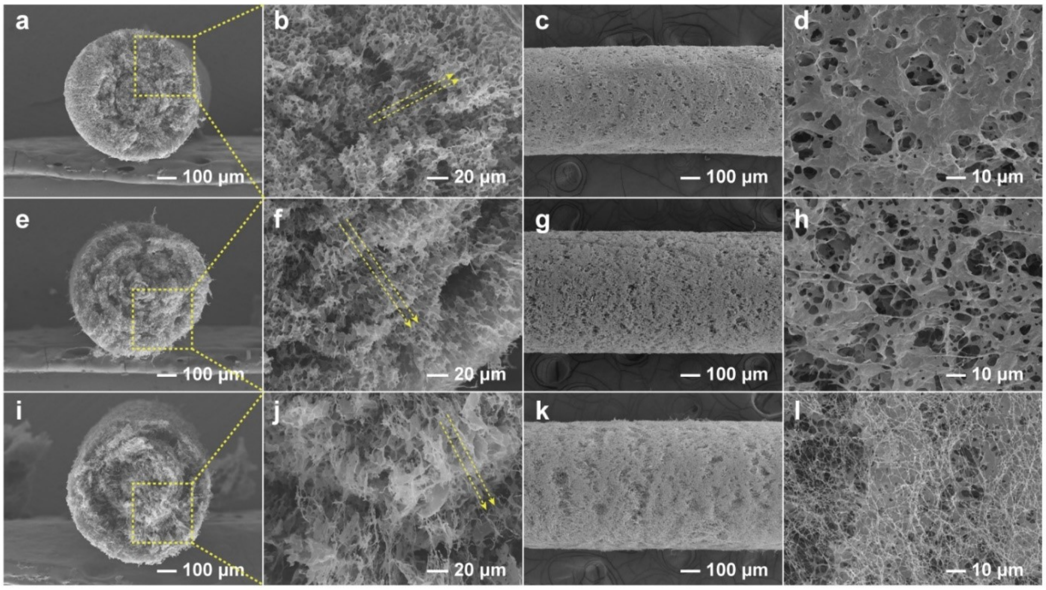

Fig. S3. SEM images of cross-sectional and surface structures of (a-d) D-MGP_1, (e-h) D-MGP_2, and (i-l) D-MGP_4 fibers.

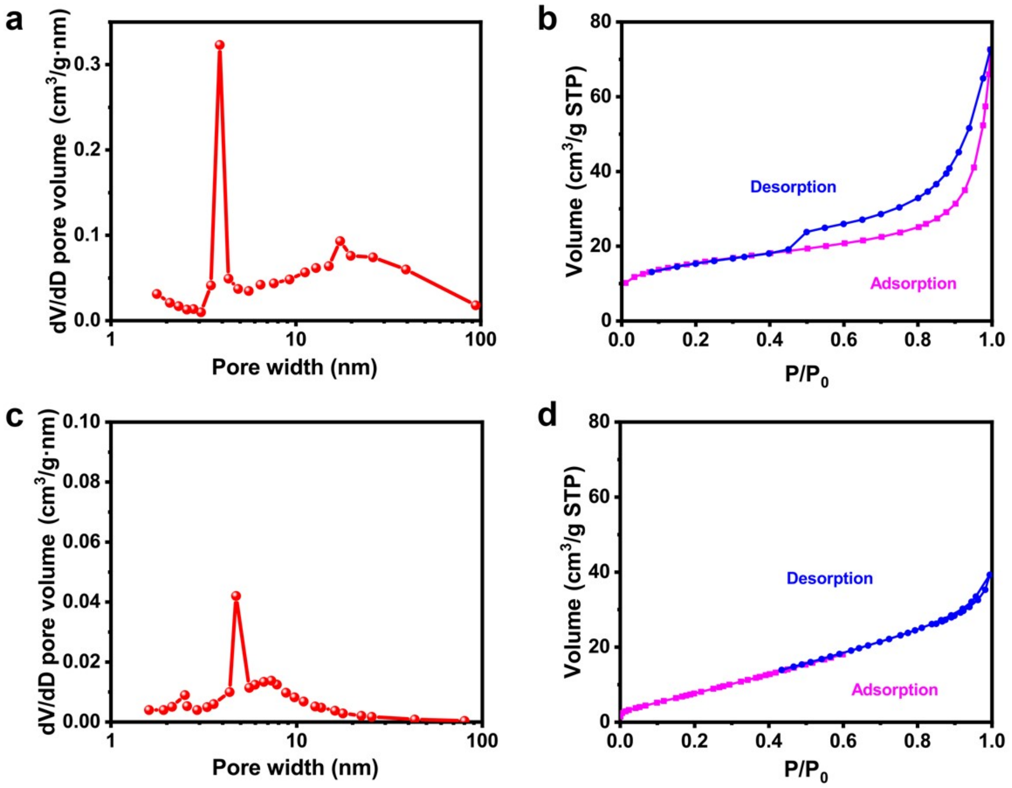

Fig. S4. Pore size distributions and the typical nitrogen adsorption and desorption isotherms of (a, b) D-MGP_3 and (c, d) U-MGP_3.

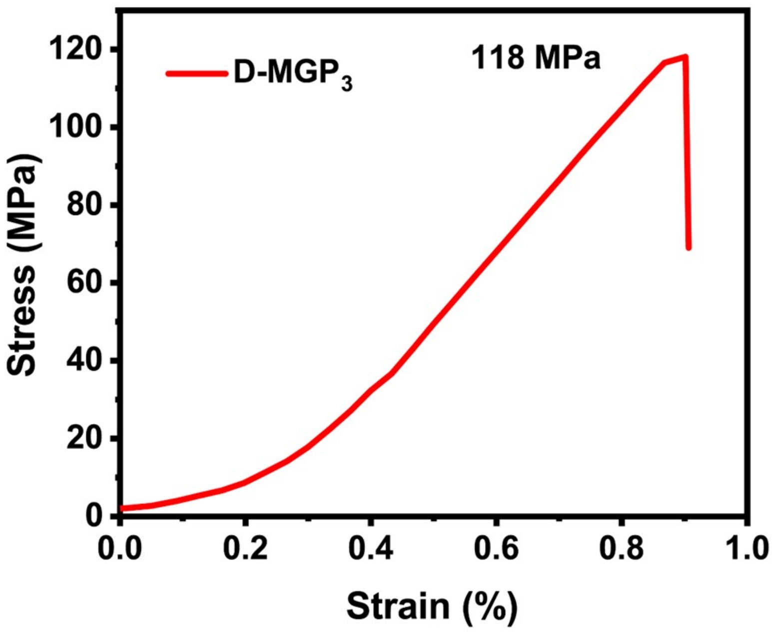

Fig. S5. Stress-strain curve of D-MGP_3.

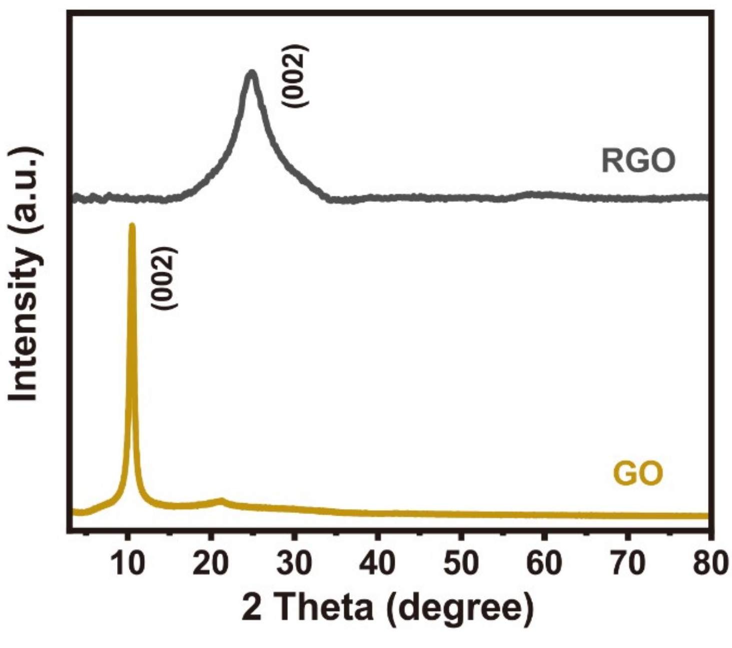

Fig. S6. XRD spectra of RGO and GO.

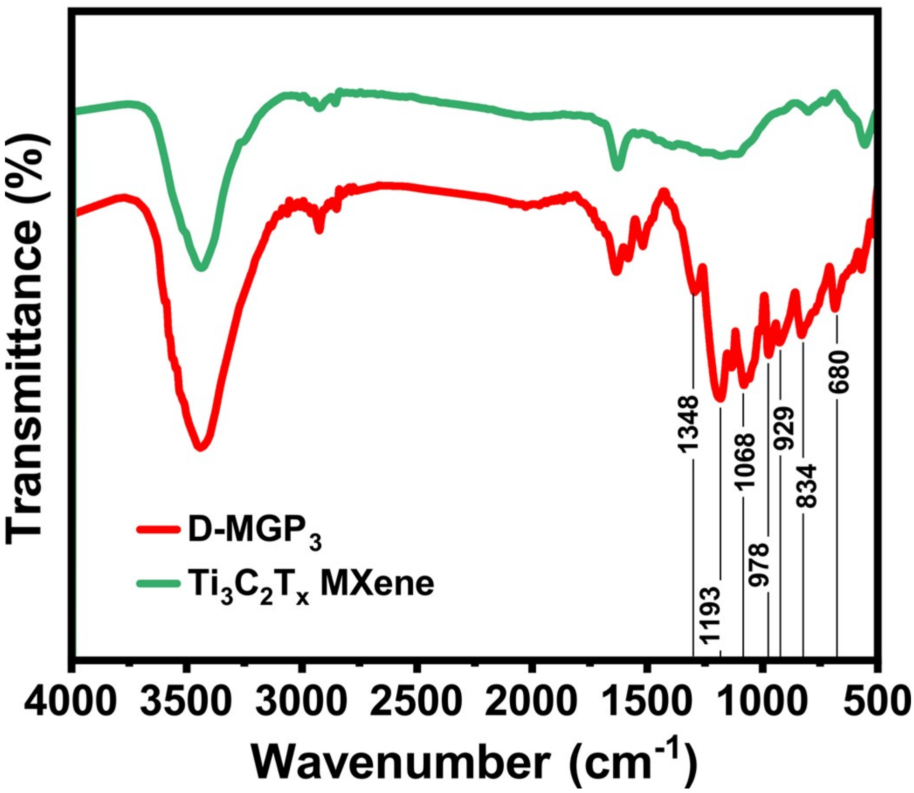

Fig. S7. FT-IR spectra of D-MGP$_3$ and MXene.

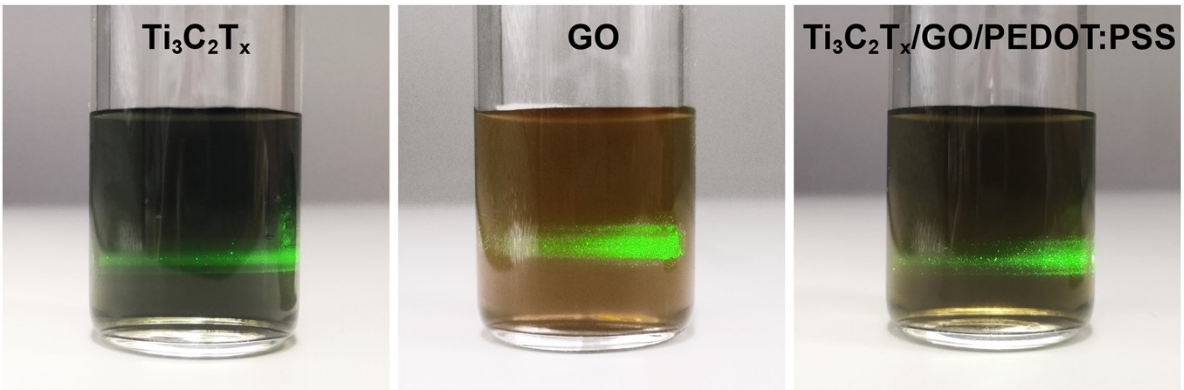

Fig. S8. Tyndall effects of $Ti_3C_2T_x$, GO, and $Ti_3C_2T_x$/GO/PEDOT:PSS suspensions.

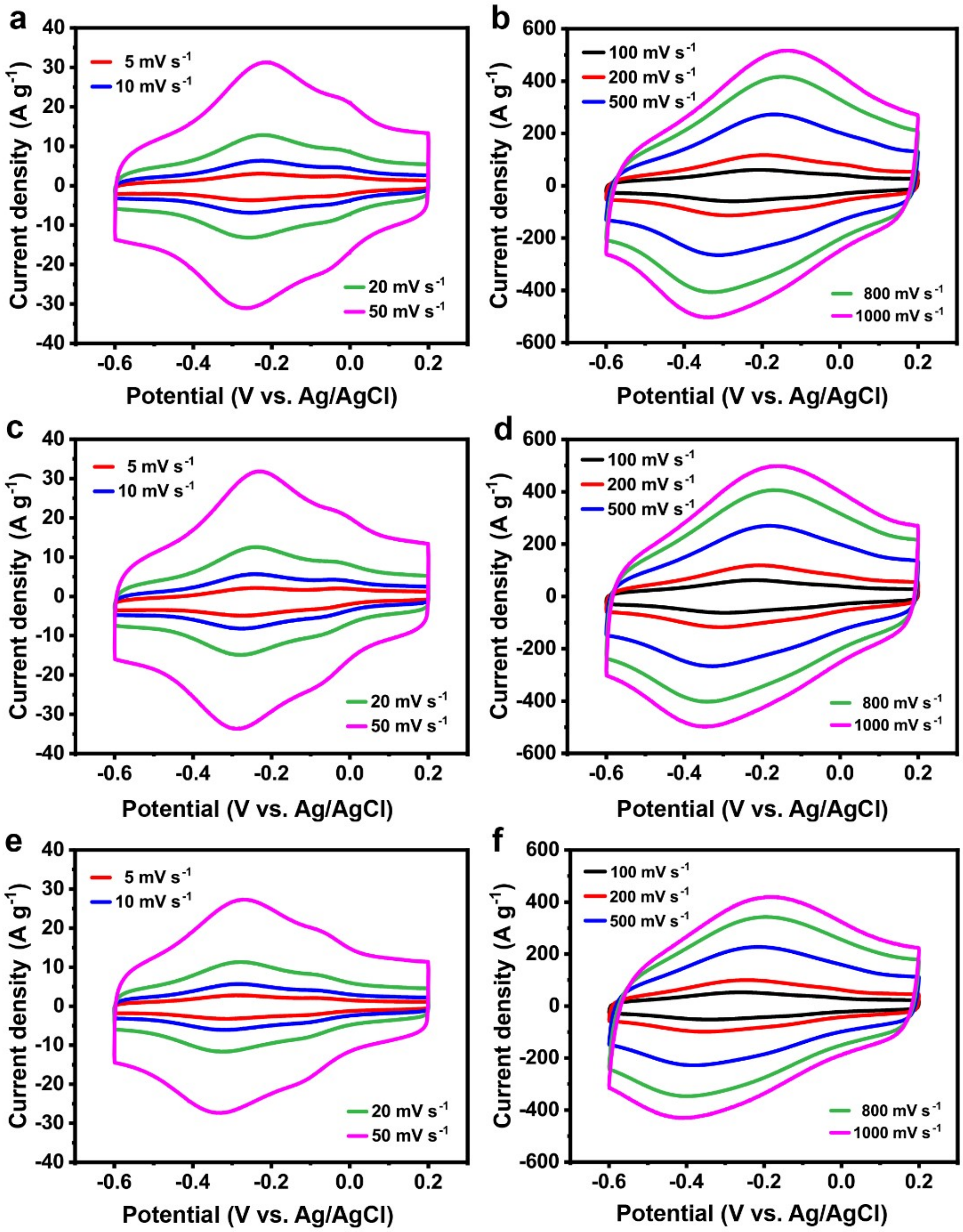

Fig. S9. CV curves of (a, b) D-MGP$_1$, (c, d) D-MGP$_2$, and (e, f) D-MGP$_4$ fibers.

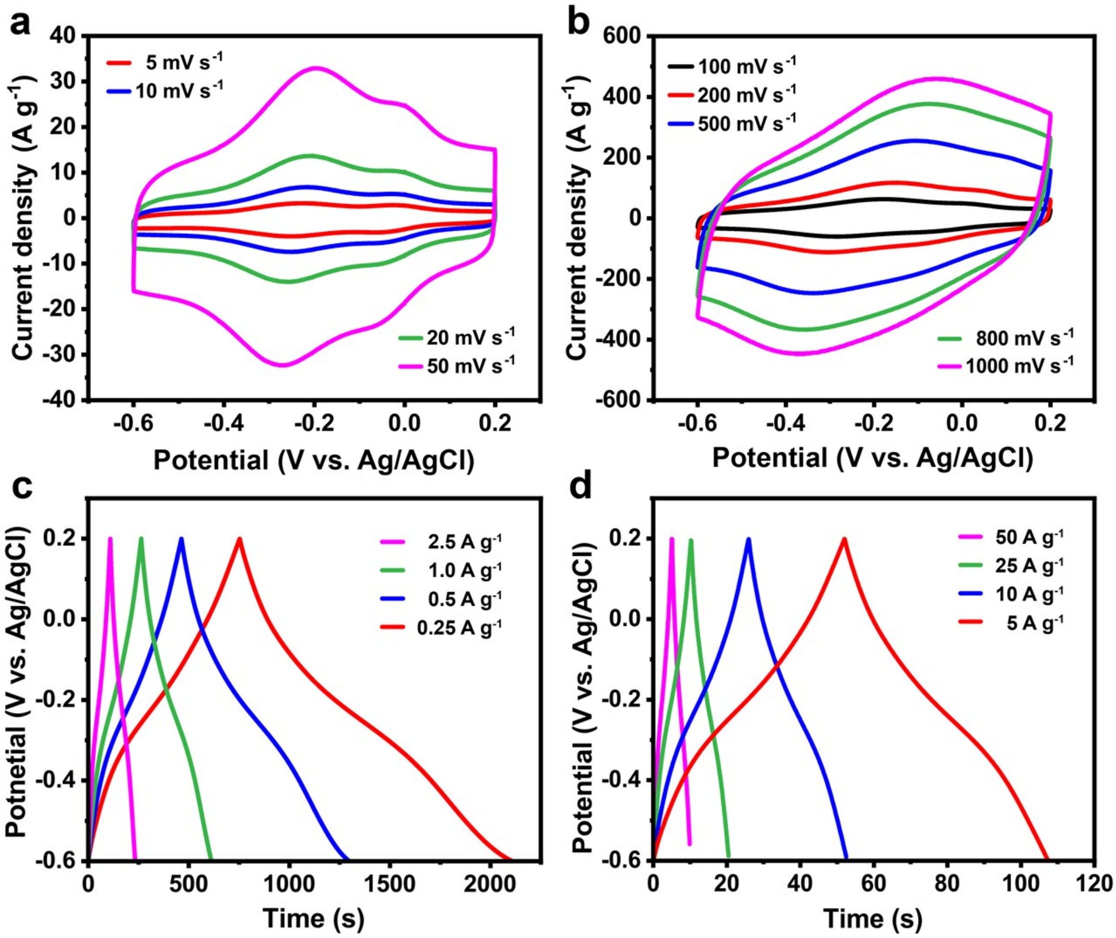

Fig. S10. (a, b) CV curves of U-MGP_3 at different scan rates; (c, d) GCD curves of U-MGP_3 at 0.25–50 A g^{-1}.

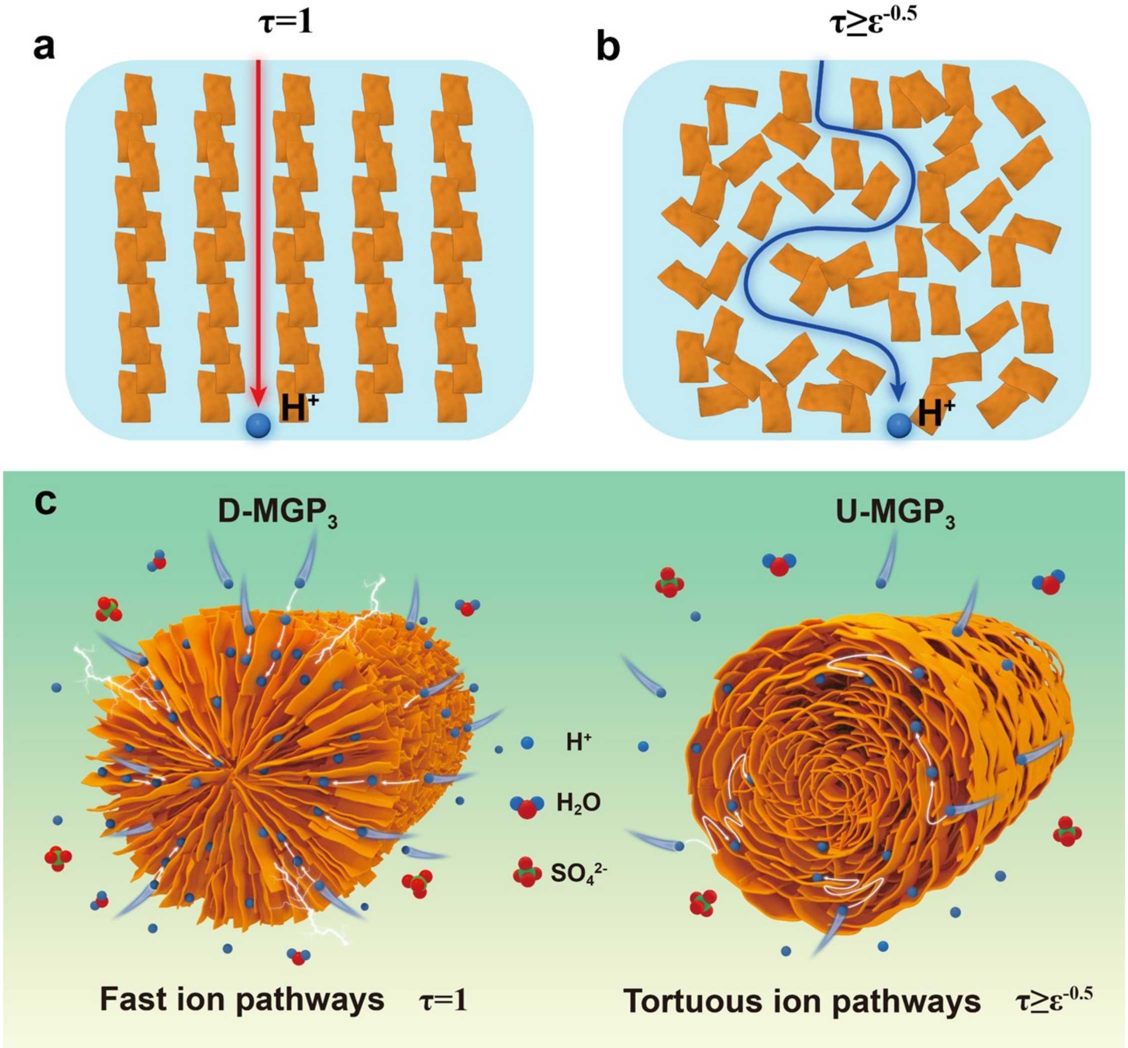

Fig. S11. Tortuosity is closely related to the size, shape, and arrangement of nanostructure in electrodes. Structures with (a) vertically aligned nanosheets and (b) randomly distributed isotropic nanosheets. (c) Schematic diagram of the ion transport pathways in D-MGP_3 and U-MGP_3.

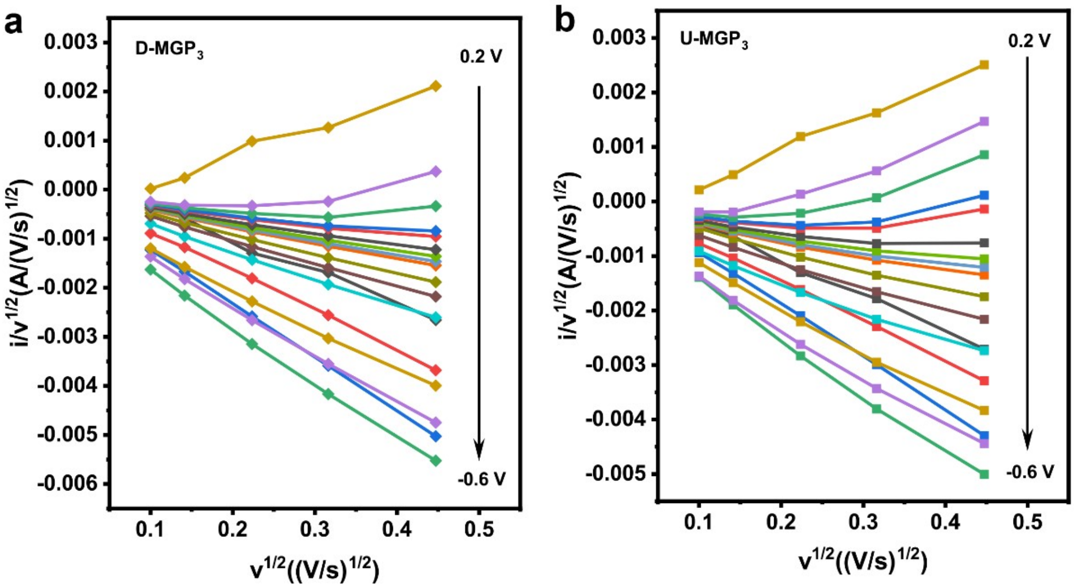

Fig. S12. Plots of $\nu^{1/2}$ vs. $i/\nu^{1/2}$ used for calculating constants k_1 and k_2 at different potentials of -0.6~0.2 V for (a) D-MGP_3, and (b) U-MGP_3 fiber electrodes.

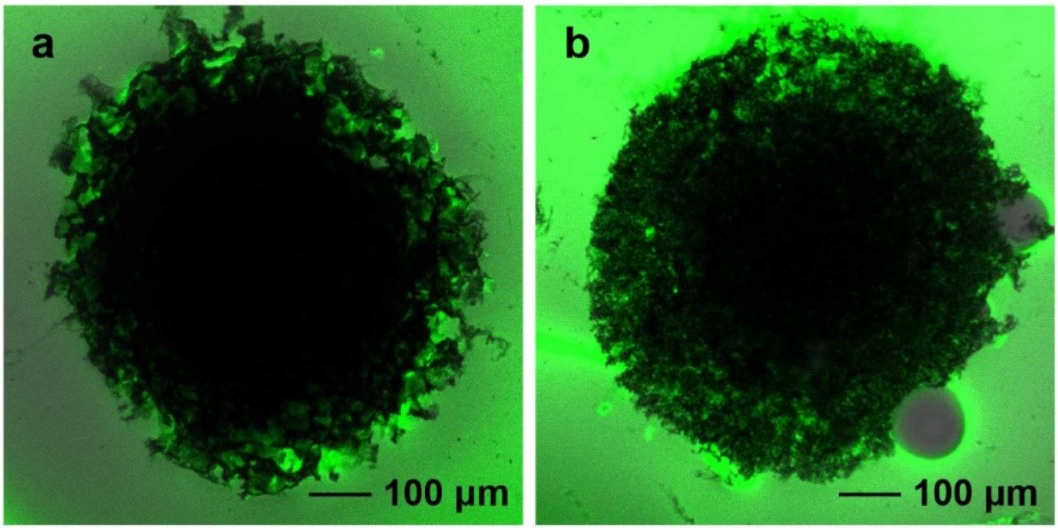

Fig. S13. Fluorescent images of the cross-sections of (a) U-MGP_3 and (b) D-MGP_3 fiber electrodes soaked in the electrolyte.

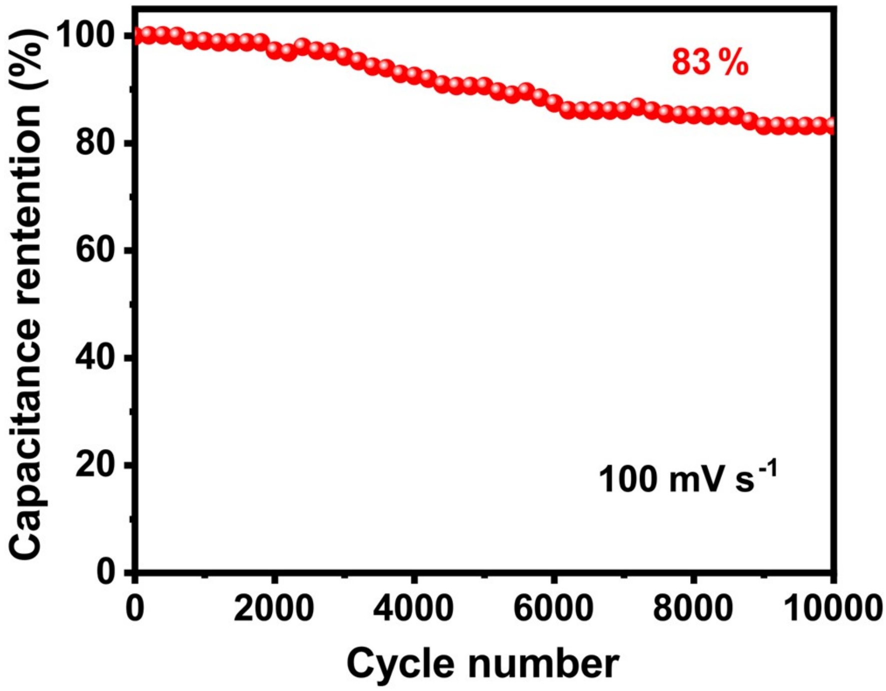

Fig. S14. Cycling stability of the fiber supercapacitor under the voltages of 0-0.8 V at a scan rate of 100 mV s^{-1} after 10000 cycles.

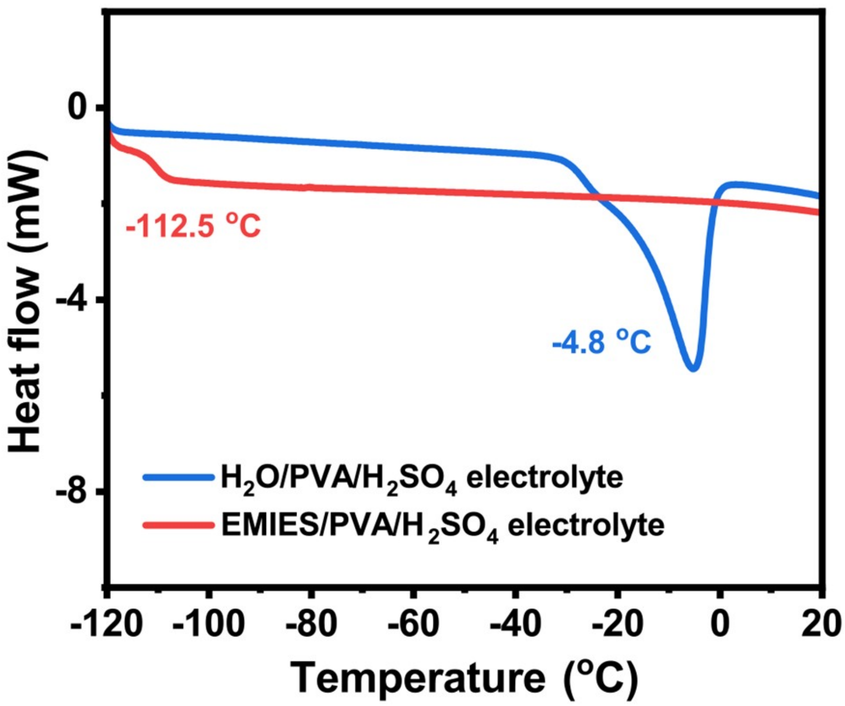

Fig. S15. DSC curves of the H_2O/PVA/H_2SO_4 electrolyte, and the EMIES/PVA/H_2SO_4 anti-freezing electrolyte.

Table S1. The simulated R_s and R_{ct} values of the hybrid fibers.

Samples	R_s（Ω）	R_{ct}（Ω）
D-MGP_1	1.315	0.761
D-MGP_2	1.091	0.545
D-MGP_3	0.579	0.284
D-MGP_4	1.763	0.579
U-MGP_3	1.021	0.718

Table S2. Comparison of electrochemical performances of the D-MGP_3 with those of other MXene-based electrodes reported.

Samples	Electrolytes	Electrochemical Performances	Rate Performances	Refs.
$Ti_3C_2T_x$	3 M H_2SO_4	380 F g^{-1} @ 2 mV s^{-1}	210 F g^{-1} @ 2000 mV s^{-1}	1
$Ti_3C_2T_x$ with alkali treatment	1 M H_2SO_4	314 F g^{-1} @ 2 mV s^{-1}	254 F g^{-1} @ 1 A g^{-1} 175 F g^{-1} @ 10 A g^{-1}	2
d-$Ti_3C_2T_x$/glycine	3 M H_2SO_4	324 F g^{-1} @ 10 mV s^{-1}	150 F g^{-1} @ 1000 mV s^{-1}	3
Few-layer $Ti_3C_2T_x$ MXene	1 M H_2SO_4	255 F g^{-1} @ 2 mV s^{-1}	150 F g^{-1} @ 200 mV s^{-1}	4
MXene/CNT yarn	3 M H_2SO_4	523 F g^{-1} @ 2 mA cm^{-2}	283 F g^{-1} @ 20 mA cm^{-2}	5
$Ti_3C_2T_x$/PPy	1 M H_2SO_4	416 F g^{-1} @ 5 mV s^{-1}	270 F g^{-1} @ 100 mV s^{-1}	6
Lignosulfonate /MXene/rGO	3 M H_2SO_4	386 F g^{-1} @ 2 mV s^{-1}	241 F g^{-1} @ 100 mV s^{-1}	7
$Ti_3C_2T_x$/rGO fiber	1 M H_2SO_4	195 F g^{-1} @ 0.1 A g^{-1}	195 F g^{-1} @ 0.1 A g^{-1} 51 F g^{-1} @ 5 A g^{-1}	8
$Ti_3C_2T_x$/PEDOT:PSS fiber	1 M H_2SO_4	258 F g^{-1} @ 5 mV s^{-1}	158 F g^{-1} @ 1000 mV s^{-1}	9
$Ti_3C_2T_x$ fiber	1 M H_2SO_4	434 F g^{-1} @ 5 mV s^{-1}	203 F g^{-1} @ 100 mV s^{-1}	10
$Ti_3C_2T_x$/rGO	3 M H_2SO_4	300 F g^{-1} @ mV s^{-1}	250 F g^{-1} @ 1000 mV s^{-1}	11
$Ti_3C_2T_x$	3 M H_2SO_4	324 F g^{-1} @ 5 mV s^{-1}	270 F g^{-1} @ 1000 mV s^{-1}	12
D-MGP_3	**3 M H_2SO_4**	**475 F g^{-1} @ 5 mV s^{-1}**	**366 F g^{-1} @ 1000 mV s^{-1}**	**this work**

References:

[1] M. R. Lukatskaya, S. Kota, Z. Lin, M.-Q. Zhao, N. Shpigel, M. D. Levi, J. Halim, P.-L. Taberna, M. W. Barsoum, P. Simon and Y. Gogotsi, *Nat. Energy*, 2017, **2**, 17105.

[2] T. Li, L. Yao, Q. Liu, J. Gu, R. Luo, J. Li, X. Yan, W. Wang, P. Liu, B. Chen, W. Zhang, W. Abbas, R. Naz and D. Zhang, *Angew. Chem., Int. Ed.*, 2018, **57**, 6115-6119.

[3] C. Chen, M. Boota, P. Urbankowski, B. Anasori, L. Miao, J. Jiang and Y. Gogotsi, *J. Mater. Chem. A*, 2018, **6**, 4617-4622.

[4] X. Wang, L. Dong, W. Liu, Y. Huang, X. Pu, J. Wang, F. Kang, J. Li and C. Xu, *J. Energy Chem.*, 2020, **48**, 233-240.

[5] Z. Wang, S. Qin, S. Seyedin, J. Zhang, J. Wang, A. Levitt, N. Li, C. Haines, R. Ovalle-Robles, W. Lei, Y. Gogotsi, R. H. Baughman and J. M. Razal, *Small*, 2018, **14**, 1802225.

[6] M. Boota, B. Anasori, C. Voigt, M. Q. Zhao, M. W. Barsoum and Y. Gogotsi, *Adv. Mater.*, 2016, **28**, 1517-1522.

[7] L. Ma, T. Zhao, F. Xu, T. You and X. Zhang, *Chem. Eng. J.*, 2021, **405**, 126694.

[8] Z. Wang, Y. Chen, M. Yao, J. Dong, Q. Zhang, L. Zhang and X. Zhao, *J. Power Sources*, 2020, **448**, 227398.

[9] J. Zhang, S. Seyedin, S. Qin, Z. Wang, S. Moradi, F. Yang, P. A. Lynch, W. Yang, J. Liu, X. Wang and J. M. Razal, *Small*, 2019, **15**, 1804732.

[10] J. Zhang, S. Uzun, S. Seyedin, P. A. Lynch, B. Akuzum, Z. Wang, S. Qin, M. Alhabeb, C. E. Shuck, W. Lei, E. C. Kumbur, W. Yang, X. Wang, G. Dion, J. M. Razal and Y. Gogotsi, *ACS Cent. Sci.*, 2020, **6**, 254-265.

[11] Z. Wu, X. Liu, T. Shang, Y. Deng, N. Wang, X. Dong, J. Zhao, D. Chen, Y. Tao and Q. H. Yang, *Adv. Funct. Mater.*, 2021, **31**, 2102874.

[12] J. Tang, T. Mathis, X. Zhong, X. Xiao, H. Wang, M. Anayee, F. Pan, B. Xu and Y. Gogotsi, *Adv. Energy Mater.*, 2020, **11**, 2003025.